Oil Shale, 2017, Vol. 34, No. 2, pp. 110–128
doi: https//doi.org/10.3176/oil.2017.2.02
ISSN 0208-189X

PETROGRAPHY AND MINERALOGY OF THE ATTARAT UM GHUDRAN OIL SHALE, CENTRAL JORDAN

VÄINO PUURA[(a)*], ALVAR SOESOO[(b)], MARGUS VOOLMA[(b)], MARE KONSA[(b)], HARDI AOSAAR[(c)]

[(a)] Department of Geology, Institute of Ecology and Earth Sciences, University of Tartu, Ravila 14A, 50411 Tartu, Estonia
[(b)] Institute of Geology, Tallinn University of Technology, Ehitajate tee 5, 19086 Tallinn, Estonia
[(c)] Eesti Energia AS, Lelle 22, 11318 Tallinn, Estonia

Abstract. *In the authors' recent papers on oil shale chemical composition and geochemical variability, as well natural gamma radiation, the significantly variable layered lithological structure of the up to 90 m thick oil shale (OS) unit of the Muwaqqar Chalk-Marl Formation (MCM), Central Jordan, was described in detail for the first time. In this work, the original results of detailed comparative petrographic and mineralogical studies of the unit and its separate layers are presented.*

The studied drill cores represent an area about 73 km^2 out of the large Attarat Um Ghudran (AUG, Attarat) deposit Maastrichtian in age. Oil shale with primary depositional structure and texture dominates. Laterally, layers, beds and interbeds of uniform composition and conditions of accumulation continue over the exploration area. Significant layering-dependent variations of chemical and mineral composition in the vertical succession of the oil shale unit occur. Petrographically, the dominating thick finely laminated uniform siliceous-carbonate mudstone (MS) oil shale intercalates with variable intervals of grain-bearing oil shale, in which interbeds of proper mudstone alternate with laminae, lenses and thin interbeds of wackestone (WS). The dominating biogenic compounds are: (i) calcite as < 5 mμ micrite forming the groundmass mudstone, and both micrite of the matrix and > 5 mμ to 1 mm grains – skeletal particles (shells and their broken fragments) in wackestone, (ii) silica as < 5 mμ particles belonging to the groundmass of mudstone and wackestone matrix, (iii) organic matter (kerogen) in the mudstone and matrix of wackestone, (iv) phosphate skeletal fragments in certain interbeds of wackestone and very fine apatite in groundmass. The clay minerals are the only possible terrigenous admixture in certain intervals. In accordance with the negative correlation between CaO and SiO_2 the layers of

* Corresponding author: e-mail *vaino.puura@ut.ee*

the dominant calcite or silica (quartz, tridymite, cristobalite) occur, whereas in MgO-rich barren interlayers dolomite may prevail and in certain P_2O_5-enriched beds/interbeds apatite or in Al_2O_3-enriched layers clay minerals occur. In the vertical succession of the oil shale unit, also quantitative proportions of principal mineral and organic (kerogen) components vary a lot. Distinct thin interlayers of carbonates with low organic matter (OM) and silica contents reflect temporary breaks and imminent recoveries of oil shale accumulation. The data serve for a further assessment and commercial development of oil shale deposits.

Keywords: *oil shale petrography, mineralogy, Maastrichtian, Attarat Um Ghudran deposit, Central Jordan.*

1. Introduction

In 2006, the Estonian power company Eesti Energia AS initiated geological investigations of oil shale (OS) deposits in Central Jordan. This led to detailed geological studies by Eesti Energia AS and the Jordan Attarat Power Company in the concession area in the southern border zone of the Attarat Um Ghudran (AUG, Attarat) deposit next to the Wadi Maghar (WM) deposit (see Fig. 1 in [1]). The uniform AUG-WM basin is located in the desert area east of the small town of Al Qattrana.

The present paper is focused on the study of the texture, structure and mineral composition of the Attarat Um Ghudran oil shale unit. Only fresh OS sequences not subjected to alterations are discussed here. The paper continues the systematic description of the AUG OS started earlier by several researchers [1–3]. Based on the classification by Hutton [4], DeWolfe et al. [5] considered the Jordanian oil shale (JOS) to belong to the family of marinites. The organic matter (OM) of JOS is described as essentially amorphous, which has been produced from marine planktonic organisms by bacterial degradation, and the product of its fossilization is dominantly presented as kerogen [6].

The richest oil shale-bearing lithostratigraphic unit in Jordan is the Muwaqqar Chalk-Marl Formation (MCM), which spans the Maastrichtian to Eocene time interval [7–10]. According to recent comprehensive microfossil biostratigraphic studies covering the whole territory of Jordan [9, 10], in the boreholes closest to the Jordan Oil Shale Energy Company's (JOSE) exploration area (at a distance of 30–70 km) (Fig. 1) the studied OS succession of AUG is most probably Maastrichtian in age. The oil shale deposits are regionally and genetically connected with the synchronous economic phosphorite deposits on the shallow marine epicontinental platform, however, separately accumulated in tectonic depression and swell facies settings, respectively [8, 10, 11].

Traditionally, Jordanian oil shales have been described as chalky marls, soft chalks, marls, marly limestones and locally microcrystalline limestones [12, 13]. Abed and Amiereh [6] established that Jordanian oil shales are not

shales but carbonates, in which the average contents of inorganic constituents are as follows: carbonates 60%, clay 6.5%, silica 3.5%, phosphate 6%, and sulphur 1.3%. Data on the mineral and chemical composition of individual samples collected from different deposits in Jordan [6, 12, 13] show the contents of these inorganic components in the samples to significantly vary. The inorganic constituents described [6] are: (i) calcite of foraminifera shells and fine-grained matrix, (ii) authigenic quartz filling the chambers of some foraminifera, composing tests of siliceous algae (supposed), and very limited detrital quartz, (iii) phosphate in pellets, intraclasts, bone, teeth, and coprolites of carbonate fluorapatite, clay minerals thought to be detrital in origin, (iv) pyrite as filling the chambers of shells and voids. Our original data below enable one to significantly update this description. Abed and Amiereh [6] and Abed and Fakhouri [7] presented detailed results of organic matter research, reporting that the phosphate in the OS from North Jordan was carbonate fluorapatite. Our X-ray diffraction (XRD) analysis of the phosphate particles in the OS of the JOSE concession area supported these statements.

During the exploration of the JOSE concession area, high recovery core sample collections from key boreholes were subjected to complex mineralogical and geochemical studies, and a layered lithological, including chemical and mineralogical, structure of the OS unit was identified.

A distinct uniformity of chemical and mineral components in the distinguished oil shale layers was identified. However, a significant variability of quantitative mineral and chemical proportions between the layers was ascertained. First, the chemical composition of separate layers is different but is principally uniform at least across the studied area [1]. Statistical analysis of the chemical data has revealed spatial regularities of elemental distribution and specificity of concentration of major and trace elements in individual layers [2]. Analysis of gamma-ray diagrams of downhole logging of wells demonstrated the layering-related distribution of elevated radioactive elements and proved the reliability of the stratigraphic scheme of the OS unit [3]. The structure, texture and mineral composition of the OS unit in general and by individual layers, as well as the appearance and patterns in the distribution of different minerals, everything in their stability and variation, are the subject of the present paper. The layering-related variation of chemical and mineral composition is a key for the further detailed interpretation of the OS accumulation conditions. On the other hand, data on compositional variations are especially important while applying the ENEFIT technologies that are focused on the ample use of Jordan's oil shale energetic potential [14].

2. Material and methods

Original results of mineralogical studies of drill cores obtained in the present Attarat Power Company exploration area are reported. The Jordan Oil Shale Energy Company owns the drill cores, detailed field and most of the laboratory data. Out of all drill cores, 12 representative cores (with very high core recovery rates) were selected for the detailed chemical [1, 2] and mineralogical studies. Altogether 385 samples from 10 geochemically and mineralogically studied drill cores were used for the present description. Throughout the sampling, sample preparation process and laboratory studies, quality control was ensured. X-ray fluorescence (XRF) analysis was conducted at the Institute of Geology, Tallinn University of Technology (TUT), with the S4 Pioneer Spectrometer (Bruker AXS GmbH), using an X-ray tube with a rhodium anode, which operated with a power of 3 kW (for details see [2, 15]). Loss on ignition was determined from 1 g of sample material at 500 and 920 °C. The average mineral composition of drill core sections, each 0.5–2 m long, as well as the insoluble residue of selected samples from different layers were studied by XRD and selectively by scanning electron microscopy integrated with energy-dispersive X-ray spectroscopy (SEM-EDS) methods. For separation of the insoluble residue from the samples, OM was oxidized by H_2O_2, carbonates and phosphates were dissolved using HCl. The mineralogical analysis of powdered samples was conducted using the HZG4 diffractometer at the Institute of Geology, TUT [2]. Complementary SEM and EDS were used to study the mode of occurrence of and genetic relations between major mineral compounds dominantly less than 1 mm in size, each forming a few to more than 50 per cent in the natural OS rock. The same technique was used to study the oxidized residue of oil shale, with OM and sulfides having been removed, as well as the bottom ash of OS test combustion. The SEM examination of uncoated rough and flat unpolished samples was carried out with the Zeiss EVO MA15 scanning electron microscope equipped with the Oxford INCA EDS detector at the Institute of Geology, TUT.

By means of SEM-EDS, the morphology, composition, and probable origin of > 5 mμ (silt and mainly fine sand) grains are described, and the overall appearance and average composition of < 5 mμ (fine silt and clay-size groundmass – OS matrix) grains are estimated. The presence of calcite, dolomite, silica (quartz, tridymite, cristobalite), apatite, clay minerals (smectite and smectite-illite) and rare sulfides in the matrix of natural OS, as well as in the IR of natural oil shale and burning test ash is interpreted from the results of XRD and SEM-EDS analyses. The mineral composition of natural OS samples is semi-quantitatively estimated (see Table, Fig. 1), integrating XRD, XRF and SEM-EDS data.

3. Results

3.1. Mineral composition and petrography of the oil shale unit and individual layers

The most abundant mineral components in oil shale layers are calcite ($CaCO_3$) and silica (SiO_2). It is compliant with the OS chemical composition [1], namely with the dominance of CaO and SiO_2 (compare Figs. 1a and 1b). Besides the overwhelming quartz, modifications of silica – cristobalite and tridymite – are abundant in layers D and C of the oil shale seam (Table and Fig. 1). SiO_2- and Al_2O_3-bearing clay minerals – smectite and smectite-illite, as well as P_2O_5-bearing carbonate-fluorapatite, are present as subordinate compounds with anomalously high contents in certain sublayers. The fifth most significant solid component of OS is the amorphous organic matter – kerogen, which is present in considerably high concentrations in all OS layers [1].

The prevalent mineral composition of the Attarat oil shale layers is of depositional origin, whereas minor diagenetic mineral aggregates occur only locally at certain stratigraphic levels. Lithologically, the OS succession is dominantly composed of alternating intervals of mudstone (MS) oil shale and wackestone (WS) oil shale, the latter with very local occurrences of packstone laminae or nests. The barren carbonate interlayers are dominantly composed of calcite-bearing crystalline dolomite rock (Fig. 1), most likely diagenetically replacing the primary limestone interlayers. However, locally the primary barren calcite-dominated limestone interlayers have survived.

Table. Semi-quantitative estimation of the average contents of main minerals in individual samples as revealed by XRD and XRF analyses of a representative core section from the Attarat Um Ghudran deposit

Layer	Depth, m		Dominating lithology	Content, mass%			
	from	to		Quartz/tridym. + cristob.	Calcite	Dolomite	Apatite
E3	59.65	61.20	MS + WS	3.2	60.3	0.3	8.7
	61.20	62.40		1.2	86.4	1.0	2.5
	62.40	63.80		0.9	74.6	0.7	6.7
	63.80	65.80		0.7	81.8	0.6	4.0
	65.80	67.80		1.0	85.3	1.0	3.2
	67.80	69.50		0.4	88.4	0.9	4.2
	69.50	70.90		0.9	85.4	1.2	3.7
E2	70.90	72.40	MS	6.4	80.2	0.6	2.6
	72.40	73.70		3.5	76.1	0.4	1.8
	73.70	75.50		3.2	54.6	0.2	4.0
E1	75.50	76.90	MS + WS	0.8	83.0	0.9	5.0
	76.90	78.70		1.7	78.1	0.7	7.8
	78.70	80.30		3.2	69.3	0.4	7.7
	80.30	81.70		2.2	81.2	1.0	3.3
	81.70	83.00		3.0	77.1	1.5	9.2

(Continuation of Table)

Layer	Depth, m		Dominating lithology	Content, mass%			
	from	to		Quartz/tridym. + cristob.	Calcite	Dolomite	Apatite
D/E	83.00	83.60	Dolomite	1.9	11.9	64.8	3.9
D	83.60	85.50	MS	8.3 30.9	10.0	21.5	5.9
	85.50	87.10		8.4 26.3	23.8	2.5	5.9
	87.10	88.40		7.9 41.7	30.9	0.8	5.8
	88.40	90.00		7.0 47.2	27.1	0.5	4.7
C	90.00	91.60	MS + WS	10.3 3.0	61.1	1.4	5.8
	91.60	93.60		11.8 12.7	35.9	0.4	8.1
	93.60	95.30		9.7 14.7	49.6	0.7	6.6
	95.30	96.90		12.0 10.2	42.9	0.4	6.4
	96.90	98.10		17.5	55.1	1.4	10.6
	98.10	99.40		9.1	42.4	2.5	29.9
B/C	99.40	99.90	Dolomite	2.0	12.6	59.1	5.6
B	99.90	101.80	MS + WS	11.0	38.2	1.5	13.9
	101.80	103.00		12.7	46.1	1.6	13.4
	103.00	104.10		10.8	54.6	1.3	9.5
	104.10	106.00		15.9	61.3	1.4	7.7
	106.00	107.80		20.8	61.4	0.9	7.2
	107.80	109.80		26.5	32.7	1.0	11.3
	109.80	111.80		27.7	27.8	3.0	12.8
	111.80	113.80		17.5	59.3	0.6	7.3
	113.80	115.80		8.3	70.8	1.1	5.3
	115.80	117.60	MS + WS; chert < 10%; apatite concretions	29.5	51.6	1.1	13.2
	117.60	119.50		20.8	66.8	0.8	7.7
	119.50	121.10		27.7	52.9	0.6	11.1
	121.10	122.80		8.0	62.1	1.6	19.7
A/B	122.80	123.60	Dolomite	1.3	9.0	67.7	4.9
A	123.60	125.50	MS + WS; chert > 10%; apatite concre-tions; calcite veins	28.3	44.1	1.7	20.2
	125.50	127.30		38.8	42.2	2.2	13.6
	127.30	128.60		20.6	57.6	0.8	11.3
	128.60	130.30		25.8	41.9	4.2	13.8
	130.30	130.80		4.3	12.7	60.9	6.0
	130.80	132.00		7.9	45.3	3.1	18.3
	132.00	133.00		46.9	35.2	1.0	6.6
	133.00	134.80		44.5	24.2	1.3	41.5

Abbreviations used: MS – mudstone, WS – wackestone, tridym. – tridymite, cristob. – cristobalite.

The prevalent depositional carbonate component of both matrix and grain phases of oil shale is calcite (Table, Fig. 1). It occurs in at least two different forms (Fig. 2): (i) volumetrically dominating fine-grained (< 5 mμ) microcrystalline micrite composing the lime-rich mudstone intervals and mudstone matrix of wackestone, (ii) organic skeleton (foraminifera shells) and

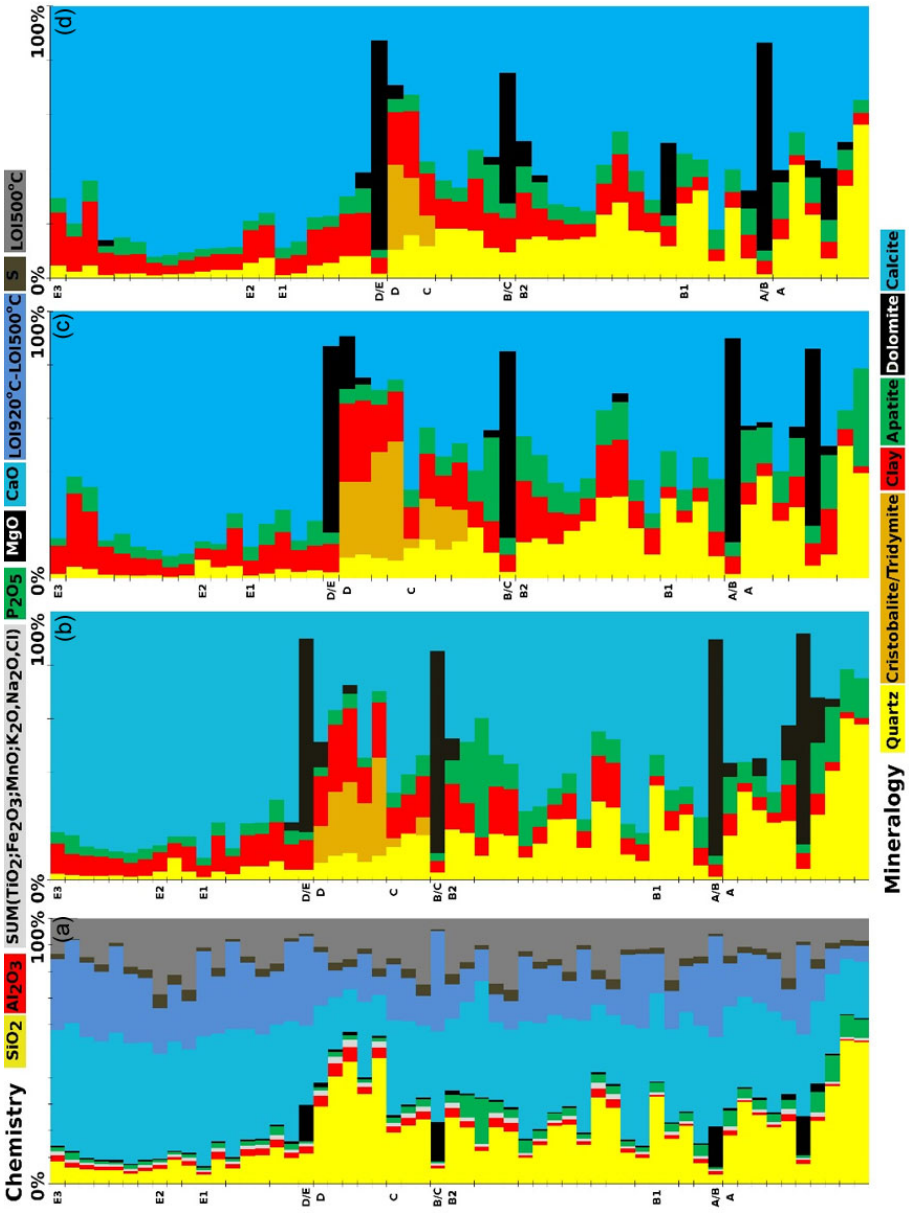

Fig. 1. The approximate average chemical and mineral composition of 0.5–2 m thick samples of OS core successions from the Attarat Um Ghudran deposit: chemical (a) and mineral (b) composition of a drill core from the western part of the concession area, and mineral composition of core samples from the southeastern (c) and northern (d) parts. The histograms are compiled using the analytical dataset (chemistry by XRF and losses on ignition and mineralogy by XRD + XRF) on the high-recovery exploration sample collection from base to top of the OS unit, the maximum thickness reaching almost 100 m.

skeletal grains (fragments, debris). In the mudstone, the < 5 mμ calcite fines are in different proportions mixed with < 5 mμ silica fines, usually with quartz, but in layers C and D partly also with tridymite and cristobalite, locally with more clay minerals, and, possibly, with roentgen-amorphous silica fines. However, only certain basic features of morphology and composition of the cryptocrystalline fine silt- to clay-size (< 5 mμ) constituents of mudstone have been studied so far. Based on general knowledge [16, 17], the finest < 5 mμ calcite and silica rounded particles, as well as carbonate and phosphate fossils and skeleton debris are of biogenic origin. The occurrence of possible processes of conversion of primary aragonite into calcite and primary opaline silica via cristobalite and tridymite into quartz remains problematic, although the locally survived coexistence of quartz and two other modifications refers to this possibility. Commonly, clay minerals are believed to refer to the terrestrial provenance. Silt- and sand-size siliceous detritus, however, were searched for, but not found during the studies. At certain levels of OS layers limited volumes of diagenetic mineralization were randomly found. In layers A, B1 and B2 rounded, few millimetre- to centimetre-size concretions and lenses or laminae of diagenetic silica (chert) and phosphate, silicified and/or phosphatized lenses, and small rounded concretions of calcite occur. Diagenetic calcite occurs occasionally as filling veins and a portion of fossil chambers and matrix pores.

From the table it can be seen that intervals of dominating mudstone with grain-bearing lamina < 10% alternate with intervals of mudstone containing 10–50% wackestone-bearing thin layers and laminae. The latter usually contain 10–50% of skeleton debris and 0.005–0.2 mm shells, randomly up to 2 mm in size. The grain and wackestone contents are estimated visually. Beds > 0.5 m thick are sampled separately. Note that the mineral composition of 0.5–2 m long samples in the true sequence of a core sequence directly visualizes the general trends (e.g. changing proportions of calcite to silica from bottom to top) and also the variability of OS compositions in aspects of presence of MS and WS alternation and dolomite interlayers.

3.2. SEM-EDS description of oil shale mineral components

SEM images of mudstone portions from the whole sequence are mostly alike, differing only due to the irregular content, size and shape of grains in the samples (Fig. 2). The largely variable contents of CaO and SiO_2 in the groundmass are semi-quantitatively estimated in selected mudstone sites by SEM-EDS. With few exceptions (layer D), CaO dominates over the other components.

The finest (< 5 μm) groundmass serves as a matrix for scattered grains > 5 μm in size. The mineral composition of grains is determined using SEM-EDS (Fig. 2c–f). Unlike the groundmass, calcite strongly dominates in the grains > 5 μm – skeletal debris, and foraminifera shells sometimes reach the

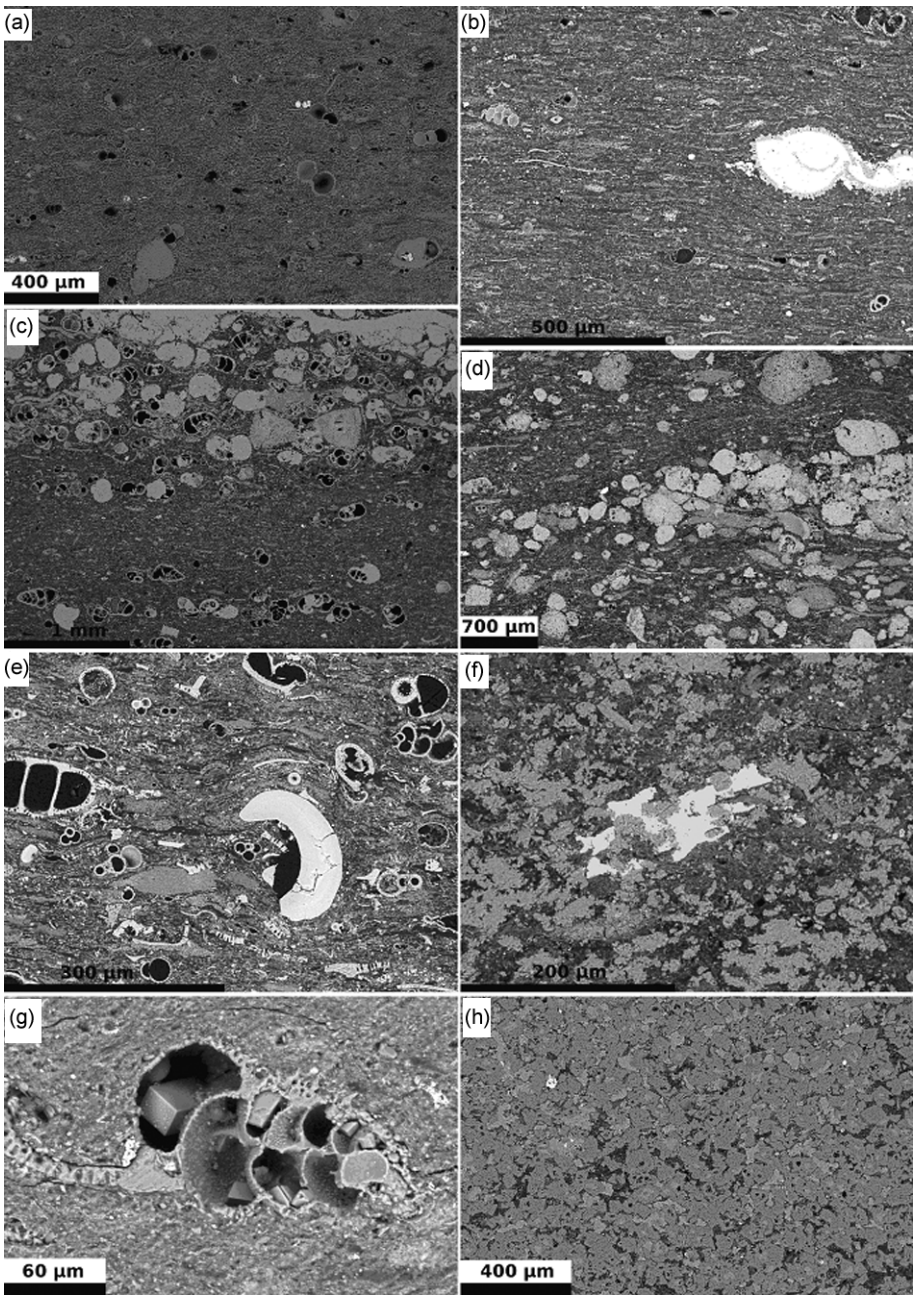

Fig. 2. (a)–(g) SEM images of selected oil shale samples demonstrating (i) structure, texture and alternation of mudstone and wackestone OS, (ii) distribution, size and composition of allochems (grains), (iii) appearance and composition of mudstone, using SEM-EDS for determination of grains and groundmass composition, (h) barren interlayer D/E (cf the average compositions of samples in Fig. 1 and Table).

size of 1–2 mm. Only apatite present in minor amounts and usually forming grains < 0.2 mm (occasionally up to 1 mm) in size is described. Extremely rare are > 5 μm sculptured grains of silica, mostly depicted as fillings in foraminifera shells and found only by enrichment of the insoluble residue (see below in 3.4).

In case of a very low (< 1%) and also low (< 10%) total content of debris and shells, the structure of the mudstone OS interbeds and lamellae may appear almost massive (Fig. 2a–d). In the process of core logging, the usual thin bedding caused by alternation of mudstone and grain-rich wackestone lamellae is visually recognized. Patterns developed as a result of the alternation of mudstone and wackestone are irregular, but to a certain degree specific for different OS layers.

The wackestone interbeds from few centimeters to several meters thick may constitute from 1 to about 70% of the rock volume in certain intervals (Fig. 2c–f). In the whole OS succession, mudstone intervals (Fig. 2a–b), however, dominate over those of wackestone. Mudstone intervals from a centimeter to almost ten meters thick alternate with parallel, continuous or discontinuous, thin (< 1 to a few mm) lamellae of wackestone interlayers, the latter can be up to a few meters thick (Fig. 2c–f, Table). Unlike calcite, abundant depositional silica is not directly visible in the presented SEM images (Fig. 2) because it is dominantly present only as mud-size (< 5 μm) particles, which together with lime mud forms intervals of almost massive or slightly laminated mudstone OS and the matrix of the wackestone intervals.

Figure 2a depicts the OS seam layer E3 comprising macroscopically almost massive fine-grained mudstone OS. Biogenic calcite grains are well-survived foraminifera tests, empty or filled with calcite micrite (here, as elsewhere, the black filling of foraminifera chambers is glue for cementing an analyte), and rare thin chips of foraminifera shells. The fine < 5 mμ groundmass is composed of dominant calcite, organic matter, minor silica and phosphate and low clay minerals, and random fine rounded pyrite.

Figure 2b illustrates layer E1, which is composed of macroscopically almost massive mudstone OS, with dominating very finely laminated micrograined (< 5 mμ) calcite and minor amounts of quartz fines (based on SEM-EDS and bulk chemistry data), and > 0.05 mm platy calcite skeleton debris and few scattered foraminifera shells. The dominant calcite groundmass contains OM and some illite-smectite. Barite randomly fills the > 0.5 mm chambers of foraminifera shells.

Figure 2c is an image of layer B2 showing a portion of thinly (on a mm scale) alternating very finely laminated OS mudstone and medium-grained wackestone, with scattered empty and micrite-filled foraminifera shells. Up right: a calcite vein. In wackestone calcite debris, grains and shells strongly dominate over phosphate debris. The very thinly laminated < 5 mμ size mudstone is composed of organic matter, calcite, clay minerals (illite-smectite), quartz, and a minor amount of apatite.

Figure 2d reveals layer B2 comprising wackestone with a lens of packstone and wavy lamina of mudstone. From 0.05 to rare 0.5 mm rounded to subrounded grains are composed of calcite micrite and rarely of apatite aggregate, fine calcite shell debris. The matrix is mudstone, which is composed of calcite, quartz, OM, clay minerals and phosphate.

Figure 2e is a SEM image of layer E2 containing wackestone OS. The unsorted grain component is composed of > 0.01 mm calcite skeletal debris to 0.2 mm calcite foraminifera tests and 0.01–0.2 mm phosphate grains/chips. The shark tooth (0.2 mm) is F-rich apatite. The matrix is mudstone composed of calcite, OM, minor quartz and clay minerals. Empty foraminifera shells are frequent.

Figure 2f shows layer D having the wackestone texture of oil shale. Specific irregular, or slightly angular, crumbly-looking grains of agglutinated calcite micrite with a minor amount of shell debris can be observed. The very fine-grained matrix of OS is rich in silica (mixture of quartz and cristobalite-tridymite) almost equal in amount to calcite. It contains organic matter, illite-smectite, with a minor amount of hidden apatite. There occur rare barite aggregates and small rounded pyrite grains.

Figure 2g presents a detailed view of layer D comprising sparry calcite developed in an empty foraminifera shell embraced by mudstone of layer D. The recrystallized shell walls consist of calcite.

Figure 2h uncovers layer D/E consisting of diagenetic crystalline dolomite. Dominant xenomorphic to idiomorphic dark gray crystals – dolomite, subordinate light gray xenomorphics – calcite, dark interstitial – fine-grained mass containing clay minerals, silica, organic matter and carbonates are present.

3.3. XRD study of the average mineral composition of natural oil shale

Chemical analyses of the collection of representative samples revealed CaO and SiO_2 to be the dominant components of OS, and XRD analyses of the same sample collection demonstrated the dominance of calcite over silica (as quartz and its modifications). The XRD study verified the regular co-existence of < 5 μm calcite and silica (quartz and other modifications) crystalline particles everywhere in the mudstone portions of OS. In addition, the XRD analyses enabled us to specify the mineral composition of the insoluble residue. Out of the 385 samples from different OS layers studied, XRD diagrams of three fresh OS samples are presented in Figure 3. The presence of calcite and quartz as well as of subordinate apatite, clay minerals (smectite and illite-smectite), apatite and rare diagenetic dolomite and also pyrite are identified in an OS sample from layer B (Fig. 3). The case is similar with the majority of samples from all other layers (Fig. 1, Table). In all samples of layer D, relatively high contents of cristobalite and tridymite and also clay minerals are detected (Table, Figs. 1 and 3). Similar mineral assemblage is occasionally found in layer C (Table, Fig. 1). Layers

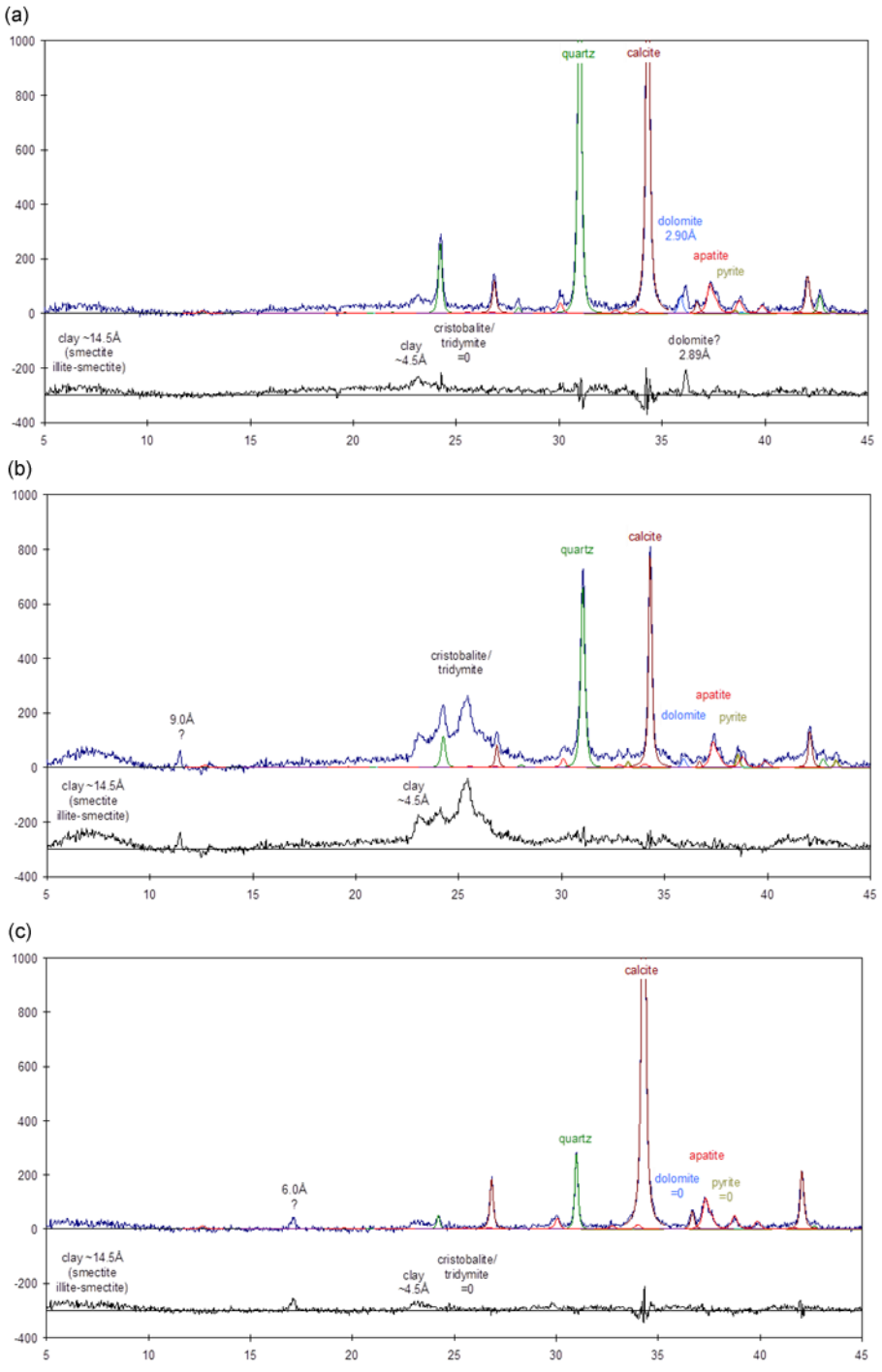

Fig. 3. XRD diagrams of fresh oil shale samples.

E1–E3 are rich in calcite and contain subordinate quartz and apatite (Table, Figs. 1 and 3). Based on the present data about layers A to E (including all the studied cores), it is apparent that contents of calcite, quartz and apatite differ by layers and sometimes within a single layer (Fig. 1). The calcite-rich layer E is most stable in terms of mineral composition. The most exceptional compositions with three modifications of silica are met in layers D and C (Table, Fig. 1).

The mineralogical patterns of the studied OS, including the insoluble residue mineralogy, in the identified layers are laterally essentially stable over the entire exploration area (Fig. 1b–d).

From Figure 3 it can be seen that the sample from layer B (Fig. 3a) has, besides the high quartz and calcite contents, a considerably low content of smectite and illite-smectite. No cristobalite or tridymite is found. Apatite, dolomite and pyrite are detectable. The sample from the SiO_2-rich OS layer D (Fig. 3b) has a remarkably high content of silica – quartz, cristobalite and tridymite, and a medium content of calcite. Apatite, dolomite and pyrite are detectable. The sample from the CaO-rich layer E (Fig. 3c) has a high content of calcite, and considerably low contents of quartz, apatite and clay minerals are characteristic. Cristobalite, tridymite, dolomite and pyrite are not detected.

3.4. XRD studies of oil shale insoluble residue

XRD diagrams of the mineral composition of the insoluble residue of the representative samples from layers B and D are depicted in Figure 4. The XRD analysis results show that the IR in layer B is composed of quartz with a small admixture of clay minerals, while in layer D it is represented by quartz, cristobalite and tridymite with a small admixture of clay minerals. The whole-rock geochemical analyses of these samples confirm the XRD findings.

3.5. SEM-EDS studies of oil shale insoluble residue

In order to specify the composition of the insoluble components of OS, and to search for possible detrital quartz and other sand grains of terrigenous nature, a selection of samples of insoluble residue from different layers was studied by SEM. The IR mainly consists of fine, < 5 μm quartz with an admixture of smectite and smectite-illite, in certain samples containing grains of diagenetic minerals – silica and randomly barite or pyrite (Fig. 4). The efficiency of the methodology used for the search of detrital quartz grains is proven by the findings of abundant 0.005–0.1 mm (coarse silt and fine sand) silica grains similar to foraminifera fossils in shape in certain IR samples (SiO_2-rich layer D) (Fig. 5a–d).

The IR sample from layer D contains silica grains < 0.1 to < 1 mm in size that dominate over other minerals, such as rare insoluble diagenetic inorganic grains of silica nodules or aggregates of barite and pyrite. Layer D

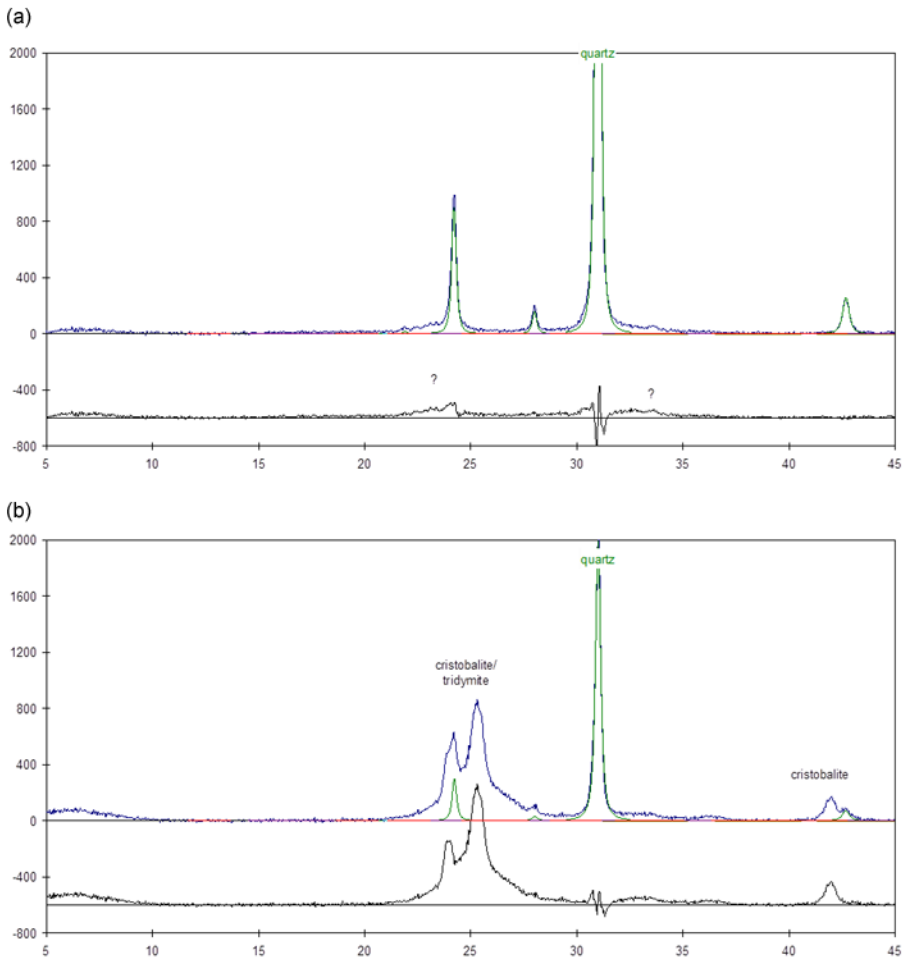

Fig. 4. XRD diagrams of (a) the insoluble residue of oil shale from layer B with a high content of quartz and no cristobalite and tridymite, and with traces of smectite, (b) the insoluble residue of oil shale from layer D having, besides quartz, a remarkably high content of cristobalite and tridymite and a low content of clay minerals.

is rich in clay minerals, but in IR no particles similar to terrigenous detrital quartz grains were found. In addition, a sample of bottom ash residue was, after oil shale burning test, subjected to leaching with HCl and the subsequent IR studies by SEM. The coarse fraction of ash residue contains silica grains of foraminifera shape (Fig. 5). A significant result of the above IR studies is that the sand-size insoluble fraction of studied samples contains only diagenetic minerals, whereas detrital quartz is not found. In the majority of IR samples sand-size quartz grains are missing, and IR is composed of < 5 mμ fine silt- and clay-size particles (mud) of siliceous matter, among which only few larger rounded grains are found (Fig. 5a). The rounded and smaller

irregular mud particles cover the grains surfaces. From Figure 5c it is seen that the mud-size particles are attached to a composite silica grain, which is shaped as the filling of test chambers.

Figure 5a depicts insoluble 50–150 mμ grains separated from the > 5 mμ IR fraction of OS. The majority of particles are composed of silica – chert. Few particles (bright in colour) are barite grains. The fine < 5 mμ particles adhere to silica grains (arrow 1). Arrow 2 points to the conchoidal fracturing of chert.

In Figure 5b the insoluble residue of OS disintegrated and agglomerated during drying is illustrated. The < 5 mμ IR fraction strongly dominates.

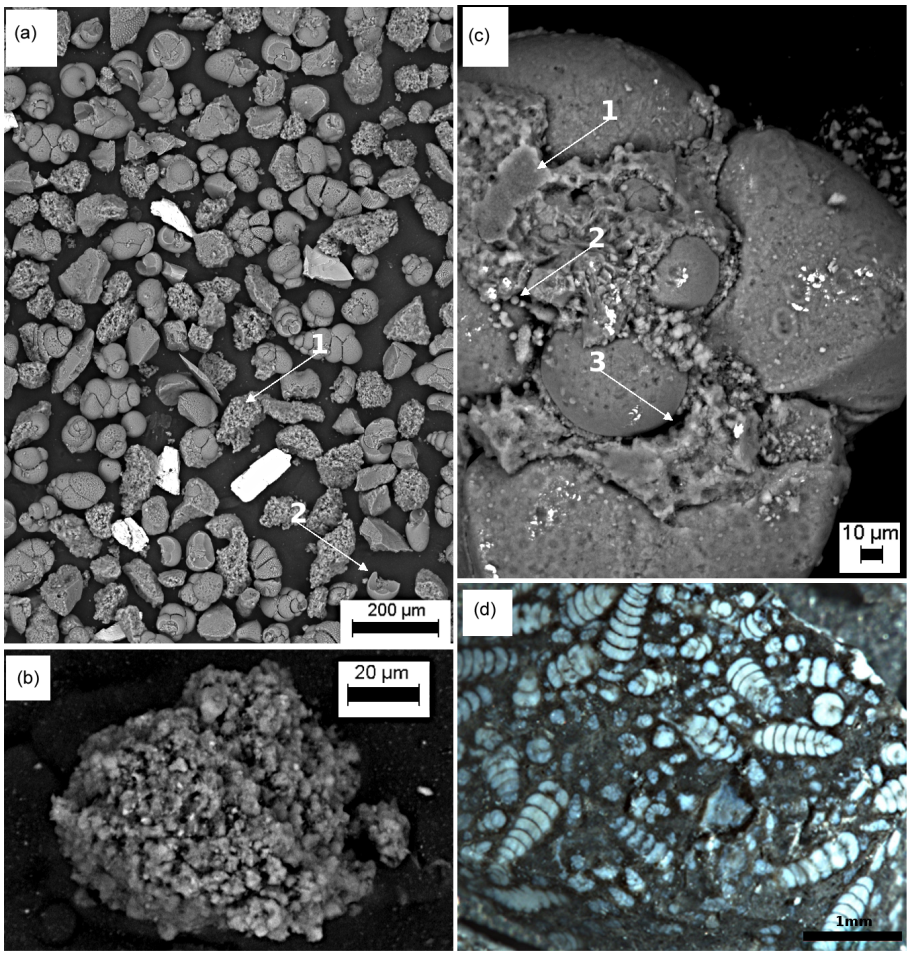

Fig. 5. SEM microphotographs of (a–c) coarse and fine inorganic particles separated from oil shale insoluble residue by HCl treatment, (d) oil shale bottom ash insoluble residue.

Figure 5c shows an insoluble grain – the chert filling the foraminifera shell, with an irregular chert filling interstitia within the fossil (arrow 1). The insoluble spherules are the probable silica particles of the < 5 mμ fraction of the mudstone matrix (arrow 2). The curved oblate voids between the segments of fossils result from the dissolution of calcite shells (arrow 3).

Figure 5d is a picture of the insoluble residue of the OS burning test ash. The OS sample is a mixture of the rock from different layers. In the fine powder of insoluble cement minerals, 0.01–1 mm silica particles shaped as fillings of foraminifera shells and their fragments are present.

3.6. Possible diagenetic mineralization of the oil shale unit

According to core logging and detailed field, geochemical and microscopic studies, diagenetic alteration processes have had a minor influence on the formation of the final geochemical-mineralogical and petrographical patterns of the Attarat Um Ghudran oil shale layers. Most of the primary depositional inorganic particles (both the mud and grain components) of OS have probably inherited their primary depositional size and shape. Dominantly, the primary depositional structures, textures and chemical composition have survived in the characteristic intervals of laminated mudstone and wackestone sections. However, so far it has not been studied how the crystalline structures of the mineral particles have survived (or changed). Possibly, the most widespread components of OS in the studied region – the calcite mud and grains – contain a large portion of recrystallized aragonite. Theoretically, the widespread silica mud is derived from amorphous opaline silica, which in time has been converted to cristobalite, tridymite, and finally to quartz [16, 17]. The formation of silica-filled foraminifera shell chambers is a trace of dissolution and local precipitation of SiO_2, which, however, is recognizable so far in the most SiO_2-rich D layer. Sparite calcite occurs randomly in the undisturbed layers and more frequently in the tectonic fracture zones.

Well-recognizable diagenetic changes of the primary depositional petrography of the oil shale seam are localized in certain laterally continuous interbeds, which mostly have a distinct stratigraphic position as well. The total thickness of such distinct beds ranges from some 2 to 7 m, of which more than a half is represented by dolomitic limestone and/or dolomite replacing the primary limestone interlayers. These beds include stratigraphic layers A/B, B/C and D/E and adjacent OS sections. The firmly identified horizons (for instance, the about 0.1 m interbeds in the middle of layer A and 0.1 to 3 m thick interlayers A/B, B/C, and D/E; Fig. 1) are well expressed in mineral composition (Table) and major elements geochemistry (Fig. 1). Partial dolomitization of some up to 3 m OS intervals next to barren interlayers is also reflected in the elevated content of MgO and dolomite (Fig. 1).

Locally, at certain levels of the lowermost oil shale layers interbeds with mm- to few cm-scale lenses, nodulous laminae and rounded nodules of chert occur. In the lower part of the OS unit, at levels enriched with phosphate debris, occasional thin lenses or small roundish nodules of phosphatized OS

are found. Also, within these intervals interbeds with random millimetre- to centimetre-size concretions of dolomite and calcite are distinguished. The listed post-depositional (diagenetic) features refer to the temporary occurrence of diagenetic processes, mostly fixed at certain levels of the OS succession. It needs to be mentioned that the variation of compositions and properties of different mineral fractions considering their specific origin during diagenesis deserves a more detailed study.

4. Conclusions

The detailed field, geochemical and mineralogical-petrographical studies of the Attarat Um Ghudrun oil shale successions and high-quality recovery sample collections from the individual OS layers established significant variations in the OS composition and internal structure in both vertical and lateral directions. This main conclusion differs from the previous understanding that the probably Maastrichtian oil shale in Jordan is uniform. Two main structural types of the original depositional oil shale alternating in the succession are defined as intervals of (i) dominating uniform, almost massive finely laminated mudstone oil shale with few lamellae of grain-bearing material, and (ii) oil shale composed of wackestone, in which mudstone as the matrix contains a variable amount (10–50, rarely 70%) of scattered grain material, which may locally be concentrated into lenses, thin beds or laminae (Table). In general, the continuous parallel primarily horizontal bedding governs the structure of the oil shale unit. Deformations and discontinuities of laminae occur on centimeter, millimeter and < 1 mm scales. In the oil shale, the contents of two main mineral components – calcite and silica (usually quartz, but in places accompanied by cristobalite and tridymite) – vary significantly, showing up reverse correlation. Two grain-size groups of rock-forming inorganic solid components differing in nature prevail in the OS matrix. First, the finest (< 5 mμ) crystalline particles of the two main minerals, quartz and calcite, locally with an admixture of clay minerals as smectite and smectite-illite and some fine apatite particles, constitute the very fine-grained (mud-size) inorganic groundmass of OS. These two main minerals are in tight intergrowth with unstructured solid organic matter, kerogen, altogether composing the pure mudstone oil shale. Second, the > 5 mμ to 0.2 mm-size, rarely to 1–2 mm-size grain fraction consists dominantly of calcite, in places with an admixture of apatite grains. The wackestone oil shale composed of mudstone as the matrix surrounding biogenic skeleton debris and foraminifera shells form over 10 mass%. Wackestone and mudstone intervals alternate throughout the OS succession. Texturally and mineralogically, the mudstone is dominantly composed of the finest, < 5 mμ calcite and silica grains, the latter documented in insoluble residue as rounded or irregular microparticles. SEM-EDS studies show that the depositional, > 5 mμ grain material of wackestone is dominantly calcite

of skeleton debris and foraminifera shells, at certain levels of OS layers also with an admixture of apatite skeletal debris. Therefore, the chemical compositions of the mudstone and grain fractions (the latter is lacking SiO_2) of OS differ significantly. Abundant grain components lower the OS grade. Interbeds with the occurrence of diagenetically transformed silica, phosphate and carbonates within OS layers may reach around 1% of the total thickness of the oil shale unit. The total thickness of dolomitized barren limestone interbeds and nearby OS may reach some 10% of the succession. The origin and technological impact of the altered OS and the barren rocks require additional studies.

Compositional differences between CaO-rich versus CaO-poor, or, respectively, SiO_2-poor versus SiO_2-rich varieties of OS are significant enough to substantially influence the technological parameters during the OS thermal treatment. According to SiO_2/CaO ratio, the prevalently limestone-dominated OS may be subdivided into SiO_2-rich, medium-SiO_2 and SiO_2-poor varieties. Locally, in layers B, D and E1–E3 interbeds enriched with Al_2O_3 (10–25% of clay minerals) are found. Within layer A, OS varieties with up to 50% apatite content occur sporadically, whereas interbeds with 5–10% apatite are also met in other OS layers.

Starting from the bottom of the OS seam, the most significant changes in OS composition occur at least at five levels. Interlayers of dolomitized limestone reflect breaks in accumulation of organic matter and pulses of diagenetic replacement of depositional calcium carbonate (aragonite and/or calcite) with diagenetic dolomite. In the middle of the OS sequence an interval of OS with extraordinary characteristics of silica (anomalous tridymite and cristobalite concentrations) occurs, covered with the barren thickest diagenetic dolomite layer. The latter corresponds to a remarkable break in OS accumulation. Starting from the base of layer E1, the composition of OS turns remarkably toward high-calcite and low-silica. In layer E2, extraordinary high OM, S and heavy trace metal concentrations appear. In lateral directions only gentle compositional variation over the entire studied area is observed. Chemical, mineralogical and gamma-ray intensity patterns enable one to recognize and follow many synchronous horizons and boundaries of change throughout the entire study area.

Acknowledgements

We thank Toivo Kallaste who conducted XRD studies at the Institute of Geology, Tallinn University of Technology. Eesti Energia AS and Attarat Power Company are thanked for the permission to use drill core materials and data for this publication.

REFERENCES

1. Puura, V., Soesoo, A., Voolma, M., Hade, S., Aosaar, H. Chemical composition of the mineral matter of the Attarat Um Ghudran oil shale, Central Jordan. *Oil Shale,* 2016, **33**(1), 18–30.
2. Voolma, M., Soesoo, A., Puura, V., Hade, S., Aosaar, H. Assessing the geochemical variability of oil shale in the Attarat Um Ghudran deposit, Jordan. *Est. J. Earth Sci.,* 2016, **65**(2), 61–74.
3. Plado, J., Ots, S., Puura, V., Aosaar, H. Interpretation of gamma-ray logs of the stratified oil shale seam in the Attarat Um Ghudran deposit, Central Jordan. *Oil Shale*, 2016,**33**(4), 340–356.
4. Hutton, A. C. Petrographic classification of oil shales. *Int. J. Coal Geol.*, 1987, **8**(3), 203–231.
5. DeWolfe, J. C., Horne, E., Morgan, C. A. *Geology and Geochemistry of the Al Lajjun Oil Shale Deposit, Central Jordan.* AAPG Conference and Exhibition, Calgary, Alberta, Canada, September 12–15, 2010.
6. Abed, A. M., Amiereh, B. S. Petrography and geochemistry of some Jordanian oil shales from North Jordan. *J. Petrol. Geol.*, 1983, **5**(3), 261–274.
7. Abed, A. M., Fakhouri, K. On the chemical variability of phosphatic particles from Jordanian phosphorite deposits. *Chem. Geol.*, 1996, **131**(1–4), 1–13.
8. Abed, A. M., Arouri, K., Amiereh, B. S., Al-Hawari, Z. Characterization and genesis of some Jordanian oil shales. *Dirasat, Pure Sciences,* 2009, **36**(1), 7–17.
9. Alqudah, M., Ali Hussein, M., Podlaha, O. G., Van den Boorn, S., Kolonic, S., Mutterlose, J. Calcareous nannofossils biostratigraphy of oil shales from Jordan. *GeoArabia*, 2014, **19**(1), 117–140.
10. Alqudah, M., Ali Hussein, M., Van den Boorn, S., Podlaha, O. G., Mutterlose, J. Biostratigraphy and depositional setting of Maastrichtian–Eocene oil shales from Jordan. *Mar. Petrol. Geol.*, 2015, **60**, 87–104.
11. Abed, A. M. The eastern Mediterranean phosphorite giants: an interplay between tectonics and upwelling. *GeoArabia*, 2013, **18**(2), 67–94.
12. Hamarneh, Y. *Oil Shale Resources Development in Jordan*. Natural Resources Authority, Hasemite Kingdom of Jordan, Amman, 1998.
13. Hamarneh, Y., Alali, J., Sawaged, S. *Oil Shale Resources Development in Jordan*. Natural Resources Authority of Jordan (updated report), Amman, 2006, 19.
14. *Enefit Outotec Technology*. www.enefit.com/en/eot (accessed 15.11.2015).
15. Voolma, M., Soesoo, A., Hade, S., Hints, R., Kallaste, T. Geochemical heterogeneity of Estonian graptolite argillite. *Oil Shale*, 2013, **30**(3), 377–401.
16. Einsele, G. *Sedimentary Basins. Evolution, Facies, and Sediment Budget*. Springer-Verlag, Berlin, Heidelberg, 2000.
17. Boggs, S. Jr. *Principles of Sedimentology and Stratigraphy*. 3rd edition. Prentice Hall, New Jersey. 2001.

Received July 4, 2016